ZIBELINE INTERNATIONAL™ PUBLISHING

ISSN: 2773-6202 (Online)
CODEN: JTIOCC

Journal of Technology & Innovation (JTIN)

DOI: http://doi.org/10.26480/jtin.01.2021.26.29

REVIEW ARTICLE

CFD-BASED STUDY ON RELATIONSHIP BETWEEN COOLING PERFORMANCE OF PULSATING FLOW AND RIB HEIGHT MOUNTED IN MINI RECTANGULAR CHANNEL

Shintaro Hayakawa[a], Takashi Fukue[a*], Hidemi Shirakawa[b] and Wakana Hiratsuka[c]

[a]Department of Mechanical Engineering, Kanazawa Institute of Technology, Hakusan City, Japan
[b]Department of Mechanical Engineering, National Institute of Technology, Toyama College, Toyama City, Japan
[c]Former student, Iwate University, Morioka City, Japan
**Corresponding Author Email: fukue@neptune.kanazawa-it.ac.jp*

ARTICLE DETAILS

Article History:

Received 15 January 2021
Accepted 19 February 2021
Available online 2 March 2021

ABSTRACT

This study aims to develop a novel water-cooled device that increases heat transfer performance while inhibiting the increase of pumping power for next-generation electronic equipment. Our previous reports have reported that the combination of the pulsating flow, which is the unsteady flow that the supply flow rate is periodically changed likes a blood in the body of human beings, and the rib has higher cooling efficiency. In this report, in order to optimize the dimensions of the ribs from the viewpoint of the cooling performance, an investigation of the pulsating flow around the rib was conducted through 2D-CFD analysis while changing the height of the rib. It was found that the level of the heat transfer enhancement was dependent on the rib height.

KEYWORDS

CFD Analysis, Heat Transfer Enhancement, Pulsating Flow, Rib Height, Water Cooling Device.

1. INTRODUCTION

Water cooling devices are widely used for heat dissipation from electronic devices that higher amount of heat is generated. There are some methods to improve water cooling performance such as an increase of flow rate itself, an increase in heat transfer area like a heat sink and mounting turbulence promotors such as ribs and vortex generators (Aliaga et al., 1994; Colleoni et al., 2013). Especially, the rib array is widely used in the narrow flow passages in order to enhance heat transfer. However, these existing methods need high performance pumps because these generates higher pressure drop. High performance pumps also cause more noise and power consumption. For the above reasons, a new cooling method that can manage both the power saving and the cooling performance is significantly needed.

The authors aim to develop a novel cooling device that can achieve high cooling efficiency. We are focusing on a pulsation flow that can be observed in blood flow in the living body (Fukue et al., 2014; Fukue et al., 2019). An effectiveness of the pulsating flow in heat transfer enhancement have been reported by several researchers such as Saito et al., Inukai et al. and Kikuchi et al. Our previous reports such as Hiratsuka have reported that the combination of the pulsating flow and the rib mounted in the mini channel that simulates water cooled devices have higher heat transfer performance than the combination of the steady flow and the rib (Hiratsuka et al., 2016; Inukai et al., 2005; Kikuchi et al., 1995; Saito and Yoshioka, 2010). The previous reports have shown the possibility of the pulsating flow as a novel technique of heat transfer enhancement. However, information about the design of the rib dimensions is not enough in order to optimize the heat transfer performance of the combination of the pulsating flow and the rib.

From these backgrounds, in this report, a relationship between the heat transfer performance by the pulsating flow and the rib height mounted in a mini-channel, that simulates a flow passage in the water-cooled device, was investigated to optimize heat transfer enhancement by pulsating flow. The research was conducted through 2D-CFD (Computational Fluid Dynamics) analysis using OpenFOAM®, that is an open-source CFD toolbox. Through the investigation, the relationship between heat transfer enhancement by the pulsating flow and the rib height was clarified.

2. ANALYTICAL METHODS

2.1 Outline of mini-channel models

Figure 1 shows an analytical model of the mini channel used in this study. This simulates two-dimensional flow passage between two parallel plates with the rib. These structure of the flow passage can be observed in some water cooling devices and finned heat sink. The dimensions of a model were as follows. The length of the channel was 150 mm. The height of the channel was 5 mm. The rib was mounted 70 mm behind the inlet of the channel in order to enhance heat transfer. The width of the rib was 2.5 mm. The rib height h was changed between 0.5 mm and 4.0 mm for evaluating the effect of the rib height on the heat transfer performance by the pulsating flow. For comparison, an analysis of the flow without the rib (hereinafter called "h = 0.0 mm") was additionally conducted. Working fluid was water.

Quick Response Code	Access this article online	
	Website: https://jtin.com.my	**DOI:** 10.26480/jtin.01.2021.26.29

Cite the Article: Shintaro Hayakawa, Takashi Fukue, Hidemi Shirakawa and Wakana Hiratsuka (2021). Cfd-Based Study on Relationship Between Cooling Performance of Pulsating Flow And Rib Height Mounted in Mini Rectangular Channel. *Journal of Technology & Innovation, 1(1): 26-29.*

The heat was generated from the bottom of the flow passage. This simulated the heat generation of the electrical chips. The heat was generated under the uniform heat flux condition. Here, in this study, in order to evaluate the level of the heat transfer enhancement in the channel itself by the rib, the rib was represented as the insulation obstacle. The heat transfer performance on the bottom was evaluated in the range of 20 times of the rib width (2.5 mm × 20 = 50 mm) at both upstream and downstream.

In this study, in order to investigate the possibility of heat transfer enhancement by pulsating flow in a mm-scale flow passage in the laminar flow condition with limited flow rate, transient laminar flow and heat transfer analysis in the low Reynolds number condition was performed. The analysis was performed by using OpenFOAM® Ver. 4.1.

As the boundary conditions of the model, the flow inlet of the model was uniform water velocity boundary. Here, when pulsating, the water velocity was changed according to the time history of the pulsating wave pattern. The outlet of the model was the free outlet boundary. Other walls and the rib surfaces were non-slip wall boundary condition. In regards to the temperature field, the flow inlet was uniform temperature condition (293.15 K), the bottom surface was uniform heat flux as described above, and the other walls was the thermal-insulation condition.

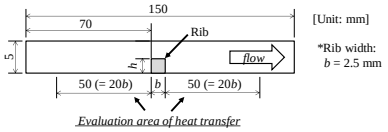

Figure 1: Dimensions of analytical model

2.2 Analytical conditions

Table 1 shows the analysis conditions. The transient CFD analysis was performed from the initial condition to the quasi-steady state. Figure 2 shows the condition of the pulsating waveform. The shape of the waveform was trapezoidal wave close to the square wave. This was the same as the previous report. The trapezoidal waveform was used from the point of the stability of the calculation. The acceleration period of the waveform was 0.5 seconds and the deceleration period was 0.5 seconds respectively in the case of 1 Hz in the pulsating frequency. For comparison, the steady flow analysis that the time-averaged flow rate was the same as the pulsating flow was also conducted. The time-average flow rate was decided by the following Reynolds number, that means the relationship between the inertial force and the viscous force of the fluid flow:

$$Re = \frac{u_c d_e}{\nu} = \frac{u_c \times 2h_e}{\nu} \quad (1)$$

Here, u_c [m/s] is the time-averaged flow velocity in the channel, d_e [m] is the hydraulic diameter in the channel, h_e [m] is the channel height and ν [m²/s] is the kinematic viscosity of the water. In the parallel plate, the hydraulic diameter can be represented as twice the clearance between the top and the bottom plates. In this report, time-averaged Reynolds number was set between 50 and 1,000.

Table 1: Analytical conditions

Flow condition	Laminar flow analysis
Analytical target	Fluid flow & Convection heat transfer
Time period of analysis	15 sec. from initial condition
Reynolds number	50 ~ 1000
Pulsating frequency	1 Hz , 0 Hz (steady)
Working fluid	Water
Height of rib	0.0 mm, 0.5 mm, 1.0 mm, 2.5 mm, 4.0 mm

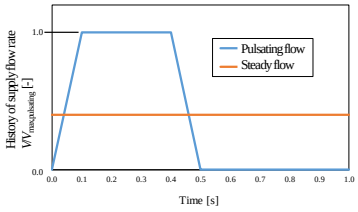

Figure 2: Condition of pulsating wave pattern

2.3 Evaluation method of heat transfer performance

The change in the heat transfer performance by the pulsating flow were evaluated by the following Nusselt number, that is the non-dimensional heat transfer performance. Here, the time-averaged local heat transfer coefficient h_x was defined as the following formula.

$$h_x = \frac{q}{T_{wall} - T_{fluid}} \quad (2)$$

where q [W/m²] is heat flux from the bottom surface, T_{wall} [K] is the bottom surface temperature and T_{fluid} [K] is inlet temperature of the working fluid. Using h_x, time-averaged local Nusselt number Nu_x and time-averaged whole Nusselt number Nu_m through the flow passage were defined as the following formulas. Here, Local Nusselt number was evaluated every 1.25 mm along flow direction.

$$Nu_x = \frac{h_x d_e}{\lambda} \quad (3)$$

$$Nu_m = \frac{1}{A}\int_A Nu_x dA \quad (4)$$

3. Analytical Results

3.1 Local Nusselt number distribution in non-rib channel

In this chapter, the effect of the pulsating flow was evaluated using the result of Re = 1000. Figure 3 shows the change of the time-averaged local Nusselt number in the case of the non-rib channel. The horizontal axis is the distance from the inlet boundary of the analytical model. In the case of the non-rib model, the local Nusselt number of the steady flow was the same as the pulsating flow. From the result, the effect of the heat transfer enhancement on the flat surface by the pulsating flow cannot be confirmed.

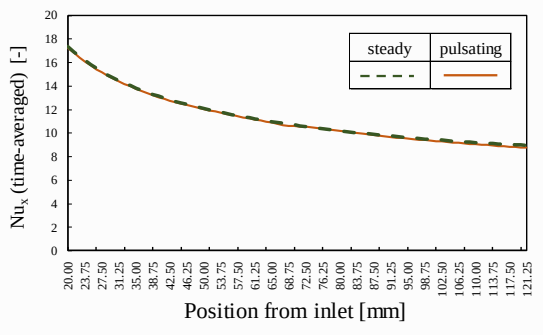

Figure 3: Time-averaged local Nusselt number distribution on bottom surface without rib

3.2 Change in the Nusselt number with rib

On the other hand, Fig. 4 shows the time-averaged whole Nusselt number of the steady flow and the pulsating flow when the rib was mounted in the channel. Here, h = 0.0 mm shows the results of non-rib model. First, the heat transfer enhancement by the rib can be confirmed regardless of the rib height and the existence of the pulsating flow. The whole Nusselt number increased in the case of both the pulsating flow and the steady flow. Furthermore, the level of the increase of the heat transfer performance was according to the rib height.

In addition, when the rib was mounted and the pulsating flow was caused, the time-averaged whole Nusselt number became higher than the result of the steady flow regardless of the rib height. In the case of h = 0.5 mm, the difference of the time-averaged whole Nusselt number between the pulsating flow and the steady flow was small. However, the height of the rib became higher, the whole heat transfer also became higher according to the rib height. Generally, the flow separation causes behind the rib and the heat transfer performance decreases. However, when the pulsating flow was caused around the rib, the counter flow was generated from the mainstream to the behind of the rib during the deceleration period. This counter flow promotes heat transfer because high temperature working fluid behind the rib can be removed. It was confirmed that the heat transfer was promoted based on this phenomenon regardless of the rib height. In addition, the level of the heat transfer enhancement by the pulsating flow is dependent on the rib height.

Figure 5 shows the distribution of the time-averaged local Nusselt number along to the flow direction. The horizontal axis shows the distance from the rib. (a) shows the distribution of the upstream side and (b) shows the distribution of the downstream side. When the pulsating flow was generated, the local Nusselt number around the rib was improved regardless of the rib height. In the downstream side, the peak value of the local Nusselt number by the pulsating flow was improved. Furthermore, the level of the local Nusselt number on the entire surface was also improved. When the higher rib was mounted, the level of the heat transfer enhancement becomes significant and there were several peak of the local Nusselt number was observed.

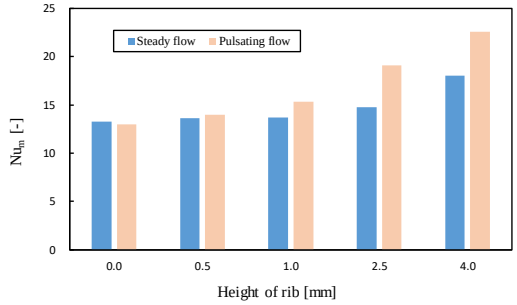

Figure 4: Comparison of average Nusselt number on the heating surface with rib between steady flow and pulsating flow

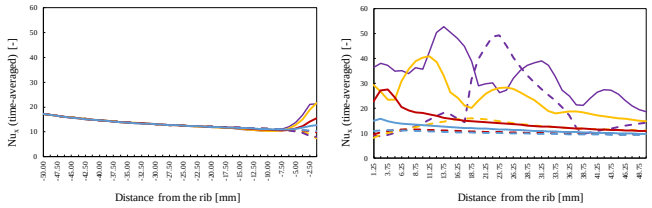

(a) Upstream side of rib (b) Downstream side of rib

rib height	steady	pulsating
0.5 mm		
1.0 mm		
2.5 mm		
4.0 mm		

Figure 5: Distribution of local Nusselt number on heating surface with rib when pulsating

3.3 Flow visualization

A mechanism of the heat transfer enhancement by the pulsating flow will be confirmed through flow visualization. Figure 6 shows the difference of the flow field between the steady flow (almost the same as the acceleration period of the pulsating flow) and the deceleration period of the pulsating flow. The left side figure shows the flow field of the steady flow and the right side is that of the deceleration period of the pulsating flow (0.1 seconds after the inlet velocity becomes 0 m/s). About the flow field of steady flow, the flow separation can be confirmed behind the rib. In addition, from the comparison of Fig. 5, the reattachment point of the flow has the peak value of the local Nusselt number. On the other hand, about the flow patten of the deceleration period of the pulsating flow, the generation of the counter flow behind the rib can be confirmed. Especially, in the case of h = 2.5 mm and h = 4.0 mm, the generation of several vortices can be confirmed. This promotes heat transfer behind the rib. In the range of this paper, the counter flow in the deceleration period can be confirmed regardless the rib height. Furthermore, when the rib height becomes higher and the area of the flow separation becomes wider, the generation of the vortices can be confirmed clearer. In this case, the vortices mix the fluid of mainstream with the fluid behind the rib. This can enhances heat transfer behind the rib. In addition, we can say that the structures of the flow in the deceleration period affects to the peak position of local Nusselt number. The impingement of the vortices to the bottom surface enhances Nusselt number and the distribution of the local Nusselt number as shown in Fig. 5 was caused.

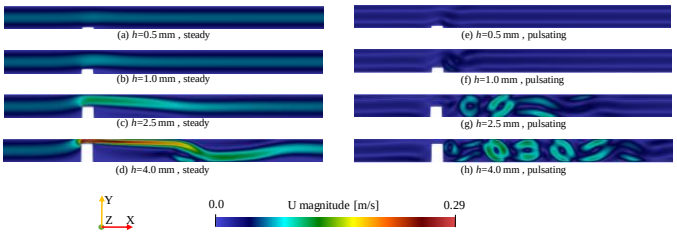

Figure 6: Difference of flow pattern between steady flow and deceleration period of pulsating flow (Re = 1000).

4. Effect of Reynolds Number

4.1 Whole Nusselt number

Finally, the relationship between time-averaged Reynolds number and Nusselt number. Figure 7 shows the relationship between the time-averaged whole Nusselt number and Reynolds number. The whole Nusselt number was increased according to the increase of Reynolds number. Here, when the height rib became higher, the level of the difference of the whole Nusselt number between the steady flow and the pulsating flow became higher. The difference was dependent on Reynolds number. We can confirm that the heat transfer enhancement was contributed by the pulsating flow with increasing Reynolds number.

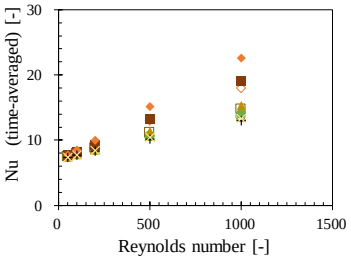

Figure 7: Relationship between whole Nusselt number and Reynolds number

4.2 Local Nusselt number

Figure 8 shows the relationship between the time-averaged local Nusselt number rear the rib and Reynolds number. (a) shows the result of h = 1.0 mm and (b) shows the result of h = 2.5 mm. From the viewpoint of the local Nusselt number, the difference of heat transfer performance between the steady flow and the pulsating flow can be confirmed regardless of the rib height and Reynolds number. Here, in the case of h = 2.5 mm, when Reynolds number becomes higher, several peak points of Nusselt number can be confirmed. On the other hand, in the h = 1.0 mm case, the peak point was one regardless of Reynolds number. The generation of vortices by the rib and the level of the inertia of the flow may affect to the level of the heat transfer enhancement.

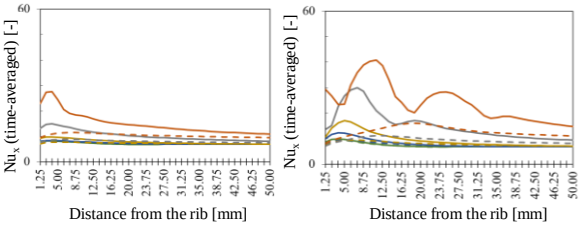

(a) h = 1.0 mm (a) h = 2.5 mm

Re	steady	pulsating
50		
100		
200		
500		
1000		

Figure 8: Distribution of time-averaged local Nusselt number on heating surface rear the rib

5. Conclusions

In this report, in order to obtain a basic database about the novel cooling devices using a combination of the pulsating flow and the rib, the relationship between the heat transfer performance by the pulsating flow and the rib height was investigated through 2D-CFD analysis. In the range of the report, we obtained the following summaries.

The heat transfer enhancement by the rib can be confirmed regardless of the rib height and the existence of the pulsating flow. Furthermore, the level of the heat transfer was according to the rib height.

In addition, about the combination of the rib and the pulsating flow, heat transfer performance became higher than the steady flow regardless of the rib height. However, the level of the heat transfer enhancement by the pulsating flow is dependent on the rib height. This is caused by the difference of the structure of the counter flow from the mainstream to the rear of the rib. The heat transfer enhancement can be confirmed regardless of time-averaged Reynolds number.

About our future research, the relationship between the rib height and the pressure drop characteristic is one of the severe problem about the application of the pulsating flow to the cooling devices. In addition, in order to evaluate a reliability of the proposed analysis, an experimental investigation will be conducted.

Acknowledgement

This work was supported by JSPS KAKENHI Grant Numbers JP16K18022, JP19K04249 and JP19K14916.

References

Aliaga, D. A., Lamb, J. P. and Klein, D. E. 1994. Convection heat transfer distributions over plates with square ribs from infrared thermography measurements, International Journal of Heat and Mass Transfer, 37-3:363-374. https://doi.org/10.1016/0017-9310(94)90071-X

Colleoni, A., Toutant, A., Olalde, G., Foucant, J. M. 2013. Optimization of winglet vortex generators combined with riblets for wall/fluid heat exchange enhancement, Applied Thermal Engineering, 50:1092-1100. https://doi.org/10.1016/j.applthermaleng.2012.08.036

Fukue, T., Hirose, K. and Yatsu, N. 2014. Basic Study on Flow and Heat Transfer Performance of Pulsating Air Flow for Application to Electronics Cooling, Transactions of The Japan Institute of Electronics Packaging, 7-1:123-131. https://doi.org/10.5104/jiepeng.7.123

Fukue, T., Shirakawa, H. and Hiratsuka, W. 2019. Basic Study on Flow and Heat Transfer Control around Heating Components in Rectangular Duct by Pulsating Flow, Proceedings of the 15th International Conference on Fluid Control, Measurements and Visualization; FLUCOME2019.

Hiratsuka, W. 2016. Possibility Investigation of Heat Transfer Enhancement in Rectangular Mini-Channels by Pulsatile Flow, Presentation Material, The 8th ASME English Presentation Competition for Japanese Students and Young Engineers.

Inukai, A., Takahashi, M., Hishida, M. and Tanaka, G. 2005. Characteristic of Heat Transportation by an Oscillatory Flow (in Japanese), Transactions of the Japan Society of Mechanical Engineers, Series B, 71-710:131-138. https://doi.org/10.1299/kikaib.71.2515

Kikuchi, Y., Ohno, Y., and Takahashi, M. 1995. Combined Forced and Free Convective Heat Transfer from a Cylinder in Pulsating Cross-Flow (in Japanese), Transactions of the Japan Society of Mechanical Engineers, Series B, 61-585:202-207. https://doi.org/10.1299/kikaib.61.1790

Saito, H. and Yoshioka, Y. 2010. Effect of pulsating Amplitude on Flow Stru cture and Associated Heat Transfer around the Flat Plate Installed in Pu lsating Duct Flow, Proceedings of the 21st International Symposium on Transport Phenomena, Kaohsiung, Taiwan.